Compatibilization of Polyethylene/Polyaniline Blends with Polyethylene-*graft*-Maleic Anhydride

T. Del Castillo-Castro,[1] M. M. Castillo-Ortega,[1] P. J. Herrera-Franco,[2] D. E. Rodríguez-Félix[1]

[1]*Departamento de Investigación en Polímeros y Materiales, Universidad de Sonora, Apartado Postal 130, Hermosillo, Sonora CP 83000, Mexico*
[2]*Unidad de Materiales, Centro de Investigación Científica de Yucatán, Calle 43, 130 Colonia Chuburná de Hidalgo, Mérida, Yucatán CP 97200, Mexico*

Received 13 November 2009; accepted 16 June 2010
DOI 10.1002/app.32971
Published online 21 September 2010 in Wiley Online Library (wileyonlinelibrary.com).

ABSTRACT: The use of compatibilizers as interfacial agents in composites can offer a convenient way to improve the mechanical properties of immiscible polymer blends. The aim of this article is to illustrate the compatibilization effect of polyethylene-*graft*-maleic anhydride (PEgMA) in blends of low-density polyethylene (LDPE) and *n*-dodecylbenzene sulfonate doped polyaniline (PANIDBSA) prepared by extrusion. Films with different compositions of the coupling agent were evaluated with optical spectroscopy and thermomechanical, electrical, mechanical, and morphological techniques. The incorporation of PEgMA into the LDPE/PANIDBSA composites resulted in an improvement of their electrical conductivity and changes in the mechanical and morphological properties of the films. When 5 wt % of the coupling agent was added to a 30 wt % of the polyaniline-containing film, the conductivity increased by more than three orders of magnitude, and the ductility also improved qualitatively. The morphology analysis also indicated that the addition of PEgMA produced a strengthening of the filler–matrix interfacial region. © 2010 Wiley Periodicals, Inc. J Appl Polym Sci 119: 2895–2901, 2011

Key words: compatibilization; composites; conducting polymers

INTRODUCTION

Polyaniline (PANI) exhibits good chemical, electrical, and optical properties, which are associated with its insulating and conducting forms. However, its insolubility in common solvents and its poor mechanical properties make its processing very difficult. In this sense, several conventional thermoplastics, such as polyethylene,[1] polypropylene,[2] nylon 12,[3] and polystyrene,[4] have been combined with PANI to obtain materials with a proper balance between the electrical and mechanical properties. Particularly, composites prepared from mixtures of low-density polyethylene (LDPE) and PANI have shown attractive properties as antistatic materials,[5] for gas-separation and ion-exchange membranes,[6] as transducers in sensor devices,[7] and for flexible electrochemical systems.[8]

The general stress–strain behavior of LDPE/PANI composites shows that the conductive polymer guest increases the rigidity of the thermoplastic host.[9,10] Understandably, the interfacial compatibility between PANI and the thermoplastic matrix is a critical requirement for obtaining good mechanical properties in these composites.

Several groups have proposed the use of compatibilizers as alternatives to strengthen the interface of immiscible LDPE/PANI blends. Yang et al.[11] found that the conductivity of PANI(dopant)$_{0.5}$/disperser/LDPE composites depended strongly on the selection of the dopant/disperser couple. Zhang et al.[12] showed that the conductivity of a ternary LDPE/PANI/ethylene vinyl acetate copolymer was higher by one order of magnitude than that of a compatibilizer-free composite. Annala and Löfgren[13] reported an improvement in the mechanical properties of polyethylene/PANI blends with the addition of functionalized metallocene polyethylene. Su et al.[10] studied the incorporation of an ethylene/acrylic acid copolymer into composites of LDPE and *n*-dodecylbenzene sulfonate doped polyaniline (PANIDBSA), and the conducting composites had a low percolation threshold of 4 wt %. The results of these studies point to the use of copolymers that contain chemical segments identical to those present in the phases and functional groups able to generate chemical and/or physical interactions with PANI.

In this article, a new approach for the compatibilization of LDPE/PANI composites is presented. The effect of the incorporation of polyethylene-*graft*-maleic anhydride (PEgMA) into blends of LDPE and PANIDBSA prepared by extrusion is evaluated. A maleic anhydride grafted polymer was considered for

Correspondence to: T. Del Castillo-Castro (terecat@polimeros.uson.mx).

© 2010 Wiley Periodicals, Inc.

this investigation on the basis of its wide use as a compatibilizer in binary immiscible blends.[14–17] The interactions between the constituents of the composite were analyzed with Fourier transform infrared (FTIR) spectroscopic measurements, ultraviolet–visible (UV–vis)/near-infrared (NIR) spectroscopy, and dynamic mechanical analysis (DMA). The electrical, mechanical, and morphological properties of the LDPE/PEgMA/PANIDBSA composites were also studied.

EXPERIMENTAL

Materials

Aniline (99.5%, Aldrich, USA) was distilled *in vacuo* before use. Ammonium persulfate (98.7%, Fermont, Mexico), *n*-dodecylbenzene sulfonic acid (99.0%, Sicursa Industrial, Mexico), acetone (99.5%, Fermont, Mexico), absolute ethanol (99.5%, Merck, Germany), LDPE (17070L, Pemex Petroquímica, Mexico), and PEgMA (3 wt % anhydride, Aldrich, USA) were used as received.

Synthesis of PANIDBSA

Aniline was chemically polymerized in the presence of dodecylbenzene sulfonate (DBSA), as described elsewhere.[18] Briefly, 130 mmol of aniline and 410 mmol of DBSA were dissolved in a 30% ethanol solution. The oxidant solution containing 60 mmol of APS in the same solvent was slowly added to the monomeric solution chilled in ice bath under a nitrogen atmosphere. The final product was precipitated with acetone and isolated by filtration in a Büchner funnel. The filter cake was washed sequentially with ethanol and deionized water several times. After that, the cake was transferred to a vessel and dried *in vacuo* at room temperature. Finally, the powder was pulverized with a mortar. The direct-current volumetric conductivity (10^{-2} S/cm) of compressed PANIDBSA powder was measured by the two-point standard method.

Preparation of the LDPE/PEgMA/PANIDBSA composites

Films with identical contents of PANIDBSA (30 wt %) and different weight ratios of LDPE to PEgMA (70/0, 65/5, 50/20, and 40/30) were obtained by mixture of the components in a Laboratory Maxwell extruder, model CS-194AV (IL, USA). The speed of rotation was 152 rpm, and the temperatures were controlled at 100 and 120°C for the rotor and the head, respectively. Composites with 2 wt % PANIDBSA and weight ratios of LDPE/PEgMA of 98/0 and 96/2 were prepared with the described conditions for the UV–vis/NIR spectroscopic analysis. Additionally, pristine films of LDPE and PEgMA were obtained also under the same conditions for comparison purposes. The composites were identified by the weight percentages of the components added to the extruder (shown in parentheses).

Characterization of the LDPE/PEgMA/PANIDBSA composites

FTIR spectroscopy of the thin composite films was performed with a GX PerkinElmer spectrometer (Buckinghamshire, England). The UV–vis/NIR absorption spectra characterization was carried out with a PerkinElmer Lambda 20 spectrophotometer (CT, USA). DMA was performed in a DMA-7 unit from PerkinElmer (CT, USA). The measurements were carried out in tensile mode at a heating rate of 5°C/min from −140 to 90°C with a fixed frequency of 1 Hz.

The volumetric electrical conductivity of the composite films was measured by the standard two-probe method. Tungsten electrodes with a diameter of 6 mm were placed on opposite sides of the film surface and in line with each other. The electrical resistances were registered in a Proam multimeter, model 602-040 (D.F., Mexico). The electrical conductivities were calculated with the contact area of the electrodes with the surface and the thickness of the film. The thickness of the film was measured with a Mitutoyo micrometer (Japan).

The mechanical properties of the composite films were measured in a tensile loading mode with a Minimat testing machine (Rheometric Scientific, NJ, USA) equipped with a load cell of 200 N at a strain rate of 1 mm/min. Rectangular samples with dimensions of 45 × 5 mm^2 were prepared. The gauge length was 25 mm. At least seven specimens from each film were tested, and the average values are reported. A typical specimen from each composition was selected, and the morphology of the failure surface was studied with a JEOL JSM-6360LV scanning electron microscope (Tokyo, Japan). The samples were gold-sputtered before the scanning electron microscopy (SEM) examination.

RESULTS AND DISCUSSION

FTIR characterization

FTIR spectroscopy of the thin films was performed to elucidate the interactions between the constituents of the composites. Figure 1 depicts the infrared (IR) spectra of the LDPE film, PANIDBSA powder, LDPE/PANIDBSA composite, LDPE/PEgMA/PANIDBSA composites with different weight ratios of LDPE to PEgMA, and PEgMA film.

Figure 1(a) shows the characteristic peaks of LDPE: (1) hydrocarbon stretching peak around 2800–3000 cm^{-1}, (2) methylene scissoring peak at 1467 cm^{-1}, and (3) methylene rocking band at 722 cm^{-1}.[19]

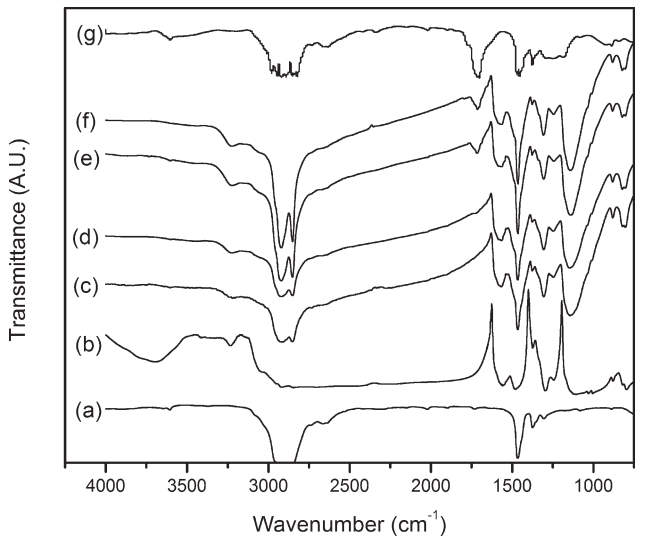

Figure 1 FTIR spectra of (a) LDPE, (b) PANIDBSA, (c) LDPE (70)/PANIDBSA (30), (d) LDPE (65)/PEgMA (5)/PANIDBSA (30), (e) LDPE (50)/PEgMA (20)/PANIDBSA (30), (f) LDPE (40)/PEgMA (30)/PANIDBSA (30), and (g) PEgMA.

The spectrum of PANIDBSA [Fig. 1(b)] showed characteristic peaks of the conducting form of PANI and those of the DBSA dopant. The band at 3229 cm^{-1} was attributed to the hydrogen-bonded N—H stretching vibration between the amine and imine sites, whereas no free N—H band was observed in the spectrum.[20] This indicated that the synthesized PANIDBSA was significantly self-associated via hydrogen bonding. The broad signal that extended from around 3000 to 1800 cm^{-1} was related to the metallic polaron state of the conducting form of PANI.[21] The bands at 1559 and 1480 cm^{-1} were due to the stretching doped C—N of the benzoid and quinoid functionalities, respectively. The significant peak around 1145 cm^{-1} was a result of the overlapping of bands assigned to functionalities, which were distinctive of the conducting form of PANI and the sulfonic group of the dopant. Furthermore, a band due to C—H *p*-substituted aromatic out-of-plane bending of PANI salt appeared at 797 cm^{-1}.

The LDPE/PANIDBSA spectrum [Fig. 1(c)] depicted the spectral contributions of the LDPE and those of the PANIDBSA. It is important to note that no new band or peak shifts appeared with respect to the individual spectra of the components; this indicated the lack of any chemical and/or physical interactions.

The spectra of PEgMA-containing composites [Figure 1(d–f)] were also dominated by the characteristic signals of LDPE and the PANI salt, however, a distinct peak was detected in the region of the carbonyl band whose intensity increased as the PEgMA content increased in the composite. This band was attributed to the carbonyl group incorporated into the system by the anhydride moiety. The spectrum of the pristine PEgMA film [Fig. 1(g)] showed the carbonyl band centered in the same position where it was positioned in the spectrum of the PEgMA-containing composites.

To further analyze the carbonyl signal, the spectral region from 1800 to 1625 cm^{-1} was magnified. Figure 2 shows the spectra of the LDPE (65)/PEgMA (5)/PANIDBSA (30), LDPE (50)/PEgMA (20)/PANIDBSA (30), LDPE (40)/PEgMA (30)/PANIDBSA (30), and pristine PEgMA films. The lack of a carbonyl signal in the spectrum of the composite that contained 5 wt % PEgMA [Fig. 2(a)] was probably due to the overlap with the broad band of PANI salt described previously and also to the low content of the coupling agent. However, as the PEgMA content was raised in the composite [Fig. 2(b,c)], a signal could be clearly distinguished at 1718 cm^{-1}, which was associated with the free C=O stretching vibration. Additionally, the spectrum of the composite with the maximum content of PEgMA [Fig. 2(c)] showed a shoulder at 1700 cm^{-1}, which was assigned to the carbonyl-bound stretching vibration. Similarly, the spectrum of the pristine PEgMA film [Fig. 2(d)] showed the carbonyl band centered in the region from 1730 to 1700 cm^{-1}, which was consistent with the spectral feature of the PEgMA-containing composites.

It is well known that the carbonyl group from an anhydride produces two bands partly overlapped in the region from 1830 to 1740 cm^{-1}. In contrast, the

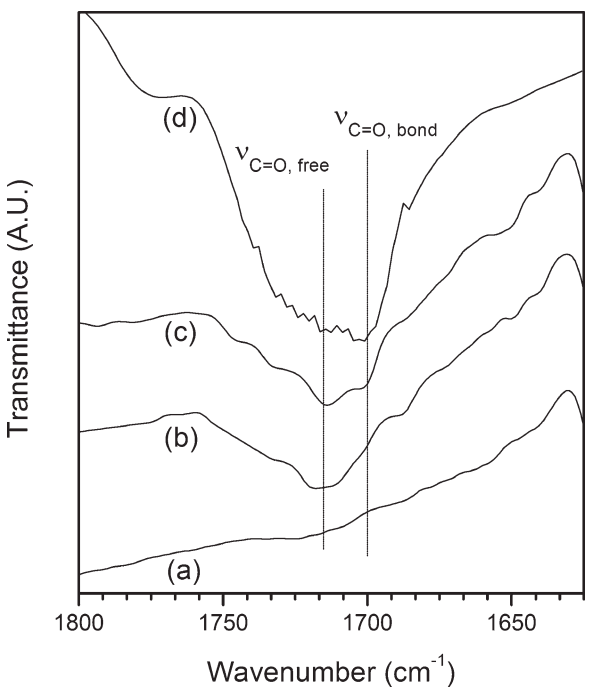

Figure 2 FTIR spectra from 1800 to 1625 cm^{-1} of (a) LDPE (65)/PEgMA (5)/PANIDBSA (30), (b) LDPE (50)/PEgMA (20)/PANIDBSA (30), (c) LDPE (40)/PEgMA (30)/PANIDBSA (30), and (d) PEgMA films.

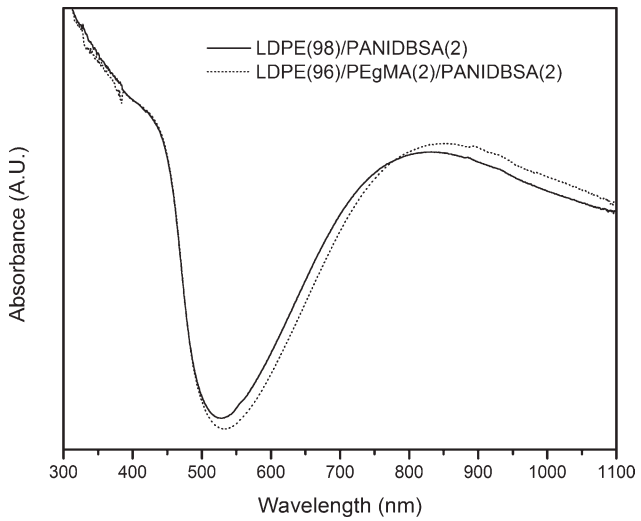

Figure 3 UV–vis/NIR spectra of LDPE (98)/PANIDBSA (2) and LDPE (96)/PEgMA (2)/PANIDBSA (2) films.

spectra of the LDPE/PEgMA/PANIDBSA composites and that of the PEgMA film showed a reduction of the carbonyl signal frequency in comparison with its position in a typical spectrum of an anhydride-containing compound. We suggest that the melt condition caused chemical changes in the anhydride moiety; this was supported by the spectral feature of the pristine PEgMA film. The formation of imide groups by the reaction of terminal amine groups of PANIDBSA and the anhydride moiety of PEgMA was neglected because the lack of the characteristic signal corresponding to the asymmetric C=O stretching (1772 cm^{-1}) of this moiety in the composite spectra. The presence of the carbonyl-bound signal suggested the existence of physical interactions, but in the case of the PEgMA-containing composites, this experimental result did not distinguish between PEgMA–PEgMA interactions and those that could have involved PEgMA and PANIDBSA. As mentioned before, the synthesized PANIDBSA was originally self-associated by hydrogen bonding [Fig. 1(b)], and this limited the analysis of PEgMA–PANIDBSA interactions from these IR data alone.

UV–vis/NIR spectra

UV–vis/NIR spectroscopy is a sensitive tool for studying the electronic state and chain conformation of PANI. Figure 3 depicts the electronic absorption spectra of the LDPE (98)/PANIDBSA (2) film and that of the LDPE (96)/PEgMA (2)/PANIDBSA (2) sample. The figure shows the typical electronic absorption spectrum of the PANI salt, which consisted of a polaron absorption near 440 nm and a broad absorption tail extending to the IR region. This last spectral feature is usually regarded as a spectroscopic sign of charge carrier delocalization in metal-like PANI. Both spectra showed similar behavior, with a slight redshift (20 nm) of the absorption tail in the PEgMA-containing composite. These spectral results indicate that the PANIDBSA presented an expanded coil-like conformation in films containing and not containing PEgMA. The expanded coil conformation of PANI allowed the increase of intrachain carrier mobility and, thus, the higher conductivity results. The UV–vis/NIR analysis demonstrated that PEgMA addition did not disrupt the intrinsic conductivity of the processed PANIDBSA.

DMA

Comparative analysis of the thermal transitions detected by the DMA technique can be a useful tool for elucidating the miscibility of phases and the presence of interfacial domains in composites. Figure 4 displays the loss tangent (tan δ) as a function of temperature for the LDPE, LDPE/PANIDBSA, and LDPE/PEgMA/PANIDBSA films.

The DMA of LDPE before melting revealed two peaks, termed the α and β transitions, in the interval of temperatures studied [Fig. 4(a)]. The α peak at 67°C was representative of the crystalline phase and originated from some type of motion in the crystals. The β peak at about −15°C is commonly attributed to the amorphous phase.[22]

With regard to the LDPE (70)/PANIDBSA (30) composite, the β-peak position on the temperature

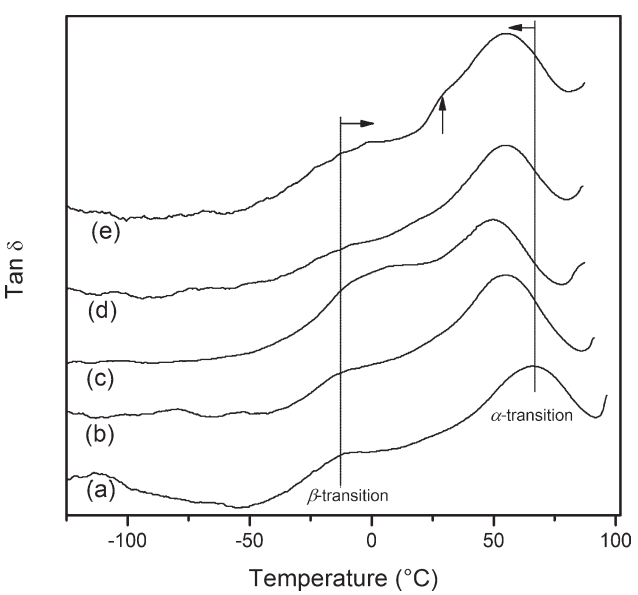

Figure 4 Temperature dependence of tan δ for (a) LDPE, (b) LDPE (70)/PANIDBSA (30), (c) LDPE (65)/PEgMA (5)/PANIDBSA (30), (d) LDPE (50)/PEgMA (20)/PANIDBSA (30), and (e) LDPE (40)/PEgMA (30)/PANIDBSA (30) films. Horizontal arrows show shifts in the thermal transition with the PEgMA concentration increasing.

TABLE I
Electrical Conductivity and Mechanical Properties of the Pristine LDPE and LDPE/PEgMA/PANIDBSA Composite Films with Different LDPE/PEgMA Weight Ratios

Film composition	Electrical conductivity ± 10%(S/cm)	Young's modulus (MPa)	Tensile strength (MPa)	Tensile deformation (%)
LDPE	$<10^{-10}$	92.1 ± 4.0	9.5 ± 0.6	156.2 ± 20.6
LDPE (70)/PANIDBSA (30)	$<10^{-10}$	112.7 ± 4.2	4.9 ± 0.2	9.8 ± 0.7
LDPE (65)/PEgMA (5)/PANIDBSA (30)	4.2×10^{-7}	77.1 ± 4.0	4.8 ± 0.2	33.7 ± 3.1
LDPE (50)/PEgMA (20)/PANIDBSA (30)	1.5×10^{-6}	77.1 ± 3.3	4.1 ± 0.2	12.3 ± 1.5
LDPE (40)/PEgMA (30)/PANIDBSA (30)	1.8×10^{-6}	85.3 ± 9.4	3.9 ± 0.2	4.9 ± 1.0

scale was not affected by the presence of PANIDBA [Fig. 4(b)]. However, the shift trend of α transition to 55°C suggested a certain degree of miscibility between the phases. When 5 wt % PEgMA was added to the composite, the β transition shifted toward higher temperatures, and a movement of the α peak to 50°C was also observed [Fig. 4(c)]. This tan δ trend confirmed the miscibility improvement with respect to the PEgMA-free film.

The films that contained 20 and 30 wt % PEgMA displayed the β transitions centered at −9 and −2°C, respectively, with both having the α peak located at 55°C [Fig. 4(d,e)]. In addition to the two transitions mentioned for the LDPE (40)/PEgMA (30)/PANIDBSA (30) composite, another small relaxation around 30°C was also detected, which may have been due to some specific transition of PEgMA, probably because of the high amount of the coupling agent in this sample.

In summary, we concluded from DMA that a mixing of phases existed in the composites with and without the coupling agent; however the effect is more significant in the PEgMA-containing films.

Electrical properties

The effect of the amount of PEgMA on the electrical properties of the melt-mixed composites was investigated. Films with a content of PANIDBSA lower than 30 wt % exhibited values of volumetric conductivity smaller than 10^{-10} S/cm, even when the coupling agent was incorporated. The degradation of PANI during the thermomechanical processing caused the poor electrical properties of the composites. However, when the amount of PANIDBSA reached 30 wt %, the coupling agent addition changed the volumetric conductivity of the composites, as shown Table I. Also, the electrical conductivity of LDPE/PANIDBSA films drastically increased with 5 wt % PEgMA, showing a moderate enhancement for higher concentrations. In general, the charge transport in a composite material depends significantly of the particle structural arrangement, conductivity, size and shape of the filler particles, and compatibility of the components. As we demonstrated before, PEgMA did not change the intrinsic electrical properties of PANIDBSA. Thus, the coupling agent played an important role in the arrangement of conducting paths in the composite.

Mechanical properties

Figure 5 shows typical stress–strain curves of the PEgMA-free film and those of the PEgMA-containing composites, and the mechanical properties are summarized in Table I. The LDPE (70)/PANIDBSA (30) composite exhibited the typical curve behavior for a brittle material. The incorporation of PANIDBSA into the LDPE matrix resulted in an enhancement of Young's modulus (22.3%) and a notorious decrease in both, the tensile strength (48.4%) and the strain to failure (93.7%). This was an expected behavior because, as we mentioned before, PANI is a brittle polymer in contrast to LDPE, which has ductile characteristics.

On the other hand, the pristine PEgMA films qualitatively demonstrated their poor mechanical properties because of the difficulty of their handling, which

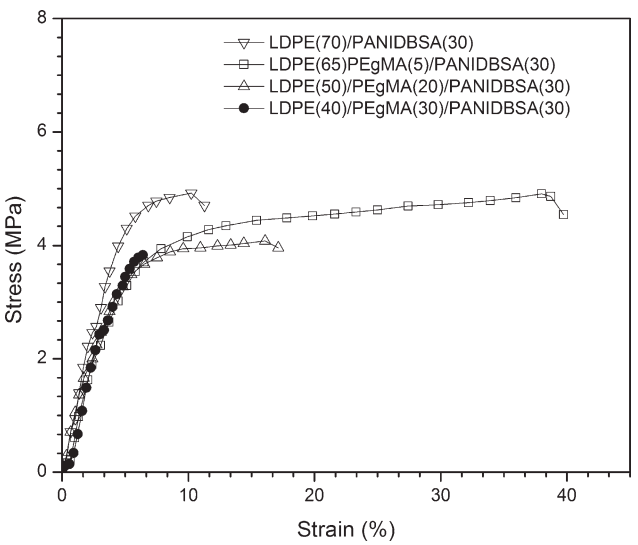

Figure 5 Stress–strain curves for films with 30 wt % PANIDBSA and LDPE/PEgMA weight ratios of 70/0, 65/5, 50/20, and 40/30.

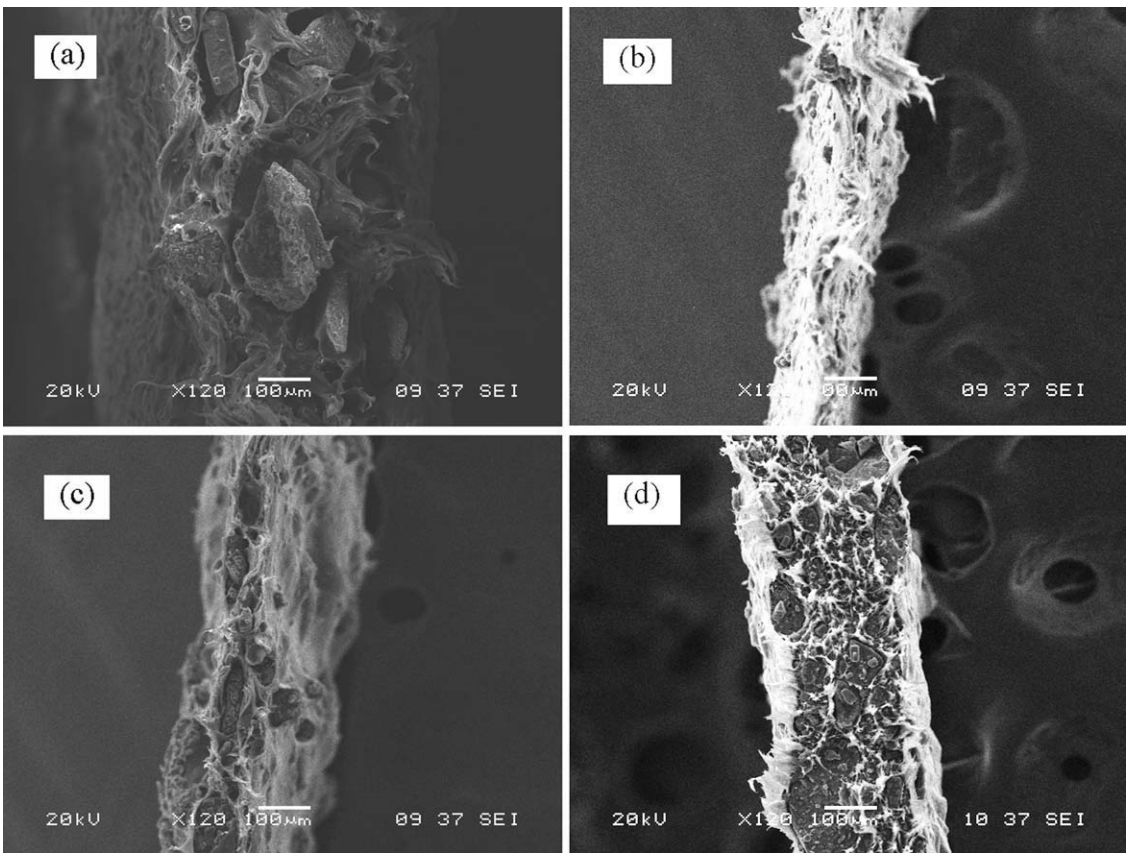

Figure 6 SEM micrographs of the surface failure of (a) LDPE (70)/PANIDBSA (30), (b) LDPE (65)/PEgMA (5)/PANIDBSA (30), (c) LDPE (50)/PEgMA (20)/PANIDBSA (30), and (d) LDPE (40)/PEgMA (30)/PANIDBSA (30) films.

made testing impossible. However, when 5 wt % PEgMA was added to the composite, an improvement in its ductility occurred compared with the behavior of the film without PEgMA. A decrease in Young's modulus (31.5%) and a substantial increase in the tensile deformation to break (243%) were observed. Considering the poor mechanical properties of PEgMA, we assumed that this enhancement in ductility was due to an improvement of the interfacial compatibility because of the presence of the coupling agent in the composites; this was consistent with previous dynamical mechanical and electrical results. Furthermore, the ductility of films with a 20 wt % content of PEgMA dramatically diminished compared to that of the composite with 5 wt % PEgMA. This result suggests that the positive compatibilization effect of the PEgMA on the ductility of the system was less significant than the negative contribution of its inherent poor mechanical characteristics. The effect was more noticeable in the film that contained 30 wt % PEgMA, as shown in its stress–strain curve.

Morphology

Figure 6 shows the morphology of the failure surface of the specimens loaded in a tensile mode. Qualitatively, the differences in the cross-section sizes of the films revealed the dissimilarity in their ductility; that is, the reduction of fracture area was proportional to the ductility of films. On the other hand, the cross section of the LDPE (70)/PANIDBSA (30) composite showed cracks between the PANIDBSA agglomerates and the matrix [Fig. 6(a)]; these indicated a weak adhesion between phases that resulted in a separation of both materials.

In contrast, the micrographs of the specimens that contained 5 and 20 wt % PEgMA [Fig. 6(b,c), respectively] revealed the presence of PANIDBSA agglomerates with matrix polymer still coating them after failure; this, thereby, indicated good adhesion between the conducting particles and the thermoplastic matrix. The morphology of the failure surface for the film containing 30 wt % PEgMA evidenced the brittle behavior shown in the tensile test [Fig. 6(d)]. Additionally, the morphology also showed that the failure stress did not produce separation in the interfacial zone. The results of the morphologic characterization were in good agreement with previous spectroscopic, thermomechanical, electrical, and mechanical results and corroborated the important role played by PEgMA in the compatibilization of the extruded composites of LDPE and PANI.

CONCLUSIONS

The use of an anhydride-based coupling agent, extensively used to compatibilize polymer blends, for example, polymers that contain amide active groups, was effectively extended to improve the electrical and mechanical properties of PANI composites. The spectral data of the LDPE/PEgMA/PANIDBSA composites indicated that the anhydride group of PEgMA chemically changed during the extrusion process and, also, that the PANI chains presented an extended coil-like conformation in the extruded films. The shift of thermal transitions of the composites strongly suggested an improvement in the miscibility of the system when the coupling agent was incorporated. The increase in conductivity and the changes in the mechanical properties of the composites with PEgMA was interpreted as a consequence of the compatibilization effect of the coupling agent. The strengthening of the interface in the PEgMA-containing composites observed by SEM corroborated the compatibilization effect of the coupling agent.

The authors thank Francisco J. C. Galván Rodríguez from the Technical Service of Pemex for providing the LDPE sample. The authors also thank Tanit Toledano for obtaining the SEM images.

References

1. Yang, J.; Rannou, P.; Planès, J.; Proń, A.; Nechtschein, M. Synth Met 1998, 93, 169.
2. Passiniemi, P.; Laakso, J.; Österholm, H.; Pohl, M. Synth Met 1997, 84, 775.
3. Shacklette, L.; Han, C. Synth Met 1993, 57, 3532.
4. Martins, C.; De Paoli, M. A. Eur Polym J 2005, 41, 2867.
5. Cardoso, M.; Lima, M.; Lenz, D. Mater Res 2007, 10, 425.
6. Tishchenko, G.; Dybal, J.; Stejskal, J.; Kudela, V.; Bleha, M.; Rosova, E.; Elyashevich, G. J Membr Sci 2002, 196, 279.
7. Jin, Z.; Su, Y.; Duan, Y. Sens Actuators B 2001, 72, 75.
8. Andersson, P.; Berggren, M.; Kugler, T. Appl Phys Lett 2003, 83, 1307.
9. Chipara, M.; Hui, D.; Notingher, P.; Chipara, M.; Lau, K.; Sankar, J.; Panaitescu, D. Compos B 2003, 34, 637.
10. Su, C.; Wang, G.; Huang, F.; Li, X. Polym Composit 2008, 29, 1177.
11. Yang, J.; Rannou, P.; Planès, J.; Proń, A.; Nechtschein, M. Synth Met 1998, 93, 169.
12. Zhang, Q.; Wang, X.; Chen, D.; Jing, X. J Polym Sci Part B: Polym Phys 2004, 42, 3750.
13. Annala, M.; Löfgren, B. Macromol Mater Eng 2006, 291, 848.
14. Chen, M.-A.; Li, H.-Z.; Zhang, X.-M. Int J Adhes Adhes 2007, 27, 175.
15. Tai, Y.; Qian, J.; Zhang, Y.; Huang, J. Chem Eng J 2008, 141, 354.
16. Sánchez-Valdes, S.; Yañez-Flores, I.; Ramos, L.; Rodriguez-Fernandez, O.; Orona-Villarreal, F.; Lopez-Quintanilla, M. Polym Eng Sci 1998, 38, 127.
17. Zhou, J.; Yan, F. J Appl Polym Sci 2004, 93, 948.
18. Castillo-Ortega, M.; Del Castillo-Castro, T.; Encinas, J.; Pérez-Tello, M.; De Paoli, M. A.; Olayo, R. J Appl Polym Sci 2003, 89, 179.
19. Hagemam, H.; Snyder, R.; Peacock, A.; Mandelkern, L. Macromolecules 1989, 22, 3600.
20. Zheng, W.; Angelopoulos, M.; Epstein, A.; MacDiarmid, A. Macromolecules 1997, 30, 2953.
21. Trchová, M.; Šeděnková, I.; Stejskal, J. Synth Met 2005, 154, 1.
22. Khanna, Y.; Turi, E.; Taylor, T.; Vickroy, V.; Abbott, R. Macromolecules 1985, 18, 1302.